

A Wiener model based closed loop FES for positional control during wrist flexion

¹ Mahendra S J, ² Vishwanath Talasila, ³ Abhilash G Dutt

¹ Research Scholar Dept of Medical Electronics, M S Ramaiah Institute of Technology, Bangalore, Karnataka, India

mahendra.j@msrit.edu

² Dept of Electronics and Telecommunication Center for Imaging Technologies, M S Ramaiah Institute of Technology, Bangalore, Karnataka, India

viswanath.talasila@msrit.edu

³ Dept of Medical Electronics, M S Ramaiah Institute of Technology, Bangalore, Karnataka, India

abhilashgdudd@gmail.com

Received: July 14, 2021. Revised: July 30, 2021. Accepted: August 1, 2021. Published: August 3, 2021

Abstract: Functional electrical stimulation is an assistive technique used to produce functional movements in patients suffering from neurological impairments. However, existing open-loop clinical FES systems are not adequately equipped to compensate for the nonlinear, time-varying behaviour of the muscles. On the other hand, closed-loop FES systems can compensate for the aforementioned effects by regulating the stimulation to induce desired contractions. Therefore, this work aims to present an approach to implement a closed-loop FES system to enable angular positional control during wrist flexion. First, a Wiener model describing the response of the wrist flexor to pulse width modulated stimulation was identified for two healthy volunteers. Second, a nonlinear PID controller (subject-specific) was designed based on the identified models to enable angular positional control during wrist flexion. Subsequently, the controller was implemented in real-time and was tested against two reference angles on healthy volunteers. This study shows promise that the presented closed-loop FES approach can be implemented to control the angular position during wrist flexion or a novelty of the work when compared with the existing work.

Key-Words: Function Electrical Stimulation, Programmable Stimulator, Wrist Flexion, Closed Loop, Nonlinear PID

I. INTRODUCTION

Functional electrical stimulation is a neuro-rehabilitative technique used to generate functional movements in patients suffering from neurological impairments [1] by applying various patterns of electrical pulses to the actuating muscle group. The clinical usefulness of FES has been demonstrated in various studies [2]. FES has played an important role in developing prostheses to assist and restore voluntary functional movements in patients after an injury [3]. FES has been used for rehabilitation that focuses on gait [4], foot drop [5] upper limb rehabilitation [6]. However, the practical use of FES in clinical scenarios is a challenging task due to the nature of the muscular system. Muscle dynamics are time-varying, nonlinear, and

susceptible to fatigue [7]. Existing open-loop clinical FES systems are not equipped to tackle this issue. The patterns used for stimulation in open-loop systems are based on empirical methods where the stimulation patterns are predefined. Continuous stimulation provided by these systems induces exaggerated contractions and rapid muscle fatigue [8]. Stimulation delivered based on feedback control can manage these challenges. These systems can use the angular position, orientation data as feedback to a controller to regulate stimulation parameters (such as pulse amplitude, pulse width, and frequency) to induce desired levels of contraction and delaying the onset of fatigue [8]. Implementing such a system requires (a) Modeling: a model to describe the response of the muscle to electrical stimulation and (b) Feedback: an external sensor to estimate the motion and use it as feedback to the controller. The performance of the closed-loop system relies upon the accuracy and simplicity of the developed model and the quality of the feedback signal.

Modeling: Developing models to describe the response of the muscle to stimulation focus on the complexity of the model and ability to capture time-varying nonlinear dynamics. Some models consider the muscle as a combination of a contractile component in series with an undamped elastic component [9], this class of models, also known as the Hill-type model, takes into account the force-length, force-velocity, and nonlinear activation dynamics while computing the response. Other techniques of modeling include the Hammerstein Wiener [10], Wiener, cascaded LNL (linear-nonlinear-linear) and black-box approaches [11]. Nonlinear models have outperformed linear models in previous experiments in terms of capturing the dynamics of the response [11]. Among nonlinear models, the Wiener model has shown the ability to fit the dynamics better than more complex cascaded LNL structures [12], but the nonlinear models proposed in [13] and [14] have superior performance.

Gathering Information for Feedback: The measurement of motion and muscle contraction enables feedback control in FES systems [15]. This data can be acquired by various means such as accelerometers, gyroscopes, EMG sensors, to name a few. Inertial measurement units are low-cost

wearable sensors that are capable of real-time estimation of movement. Sensor fusion algorithms improve the measure of movement from IMU by incorporating the short-term accuracy of gyroscopes and the long-term accuracy of accelerometers. The sensor fusion techniques differ by the mathematical framework, and the filters used for combining the data (Kalman filters, complementary filters, and sliding mode observers) [16, 17].

This work aims to present an approach to implement a closed-loop FES system towards enabling angular positional control during wrist flexion by effectively regulating the stimulation pulse width (constant stimulation pulse amplitude). A Wiener model was estimated to identify the response of the wrist flexors to the pulse width modulated stimulation on healthy volunteers. This model was selected as the plant model in the PID design. A nonlinear PID system has been designed to compensate for the nonlinearities in the model. Angular position estimated from the accelerometer and gyroscope readings using a complementary filter algorithm is used to provide feedback to the controller. The controller was tested on healthy volunteers, and the performance was quantified. Section 2 of this work presents the methods undertaken to (a) identify the dynamics of wrist flexors and (b) design and test the nonlinear PID system. In Section 3, the results of the model identification are presented. Subsequently, the performance of the nonlinear PID controller is reported. The findings and limitations of this work are discussed in Section 4 before concluding this work in Section 5.

II. METHODS

A. Identification of the Response of Wrist Flexors to Electrical Stimulation

Before designing the nonlinear PID controller, experiments were conducted on healthy volunteers to identify a model representing the response of the wrist flexors to electrical stimulation with varying pulse width while keeping the pulse amplitude constant, hence making the proposed approach better than the neural network approach or the constant amplitude of the neural network are not accurate for the computed amplitude.

Participants: Two healthy volunteers (two males, aged 24 & 58 years respectively, and BMI: 21.6 and 24.8 kg/m²) were considered for the experiments after informed consent. The volunteers in this work are identified as S1,S2. It was ensured that the subjects had no skin allergies, no metallic or electrical implants, and no known cardiovascular condition.

Experimental Process

A custom designed programmable current-controlled functional electrical stimulator was used to provide electrical stimulation through surface electrodes. The device is supported by an STM32F446 (STMicroelectronics) microcontroller, which facilitates the generation of stimulation pulses and acquisition of data from an inertial

measurement unit (MPU6050, six axes, gyroscope + accelerometer). Trains of biphasic rectangular pulses were applied at a fixed frequency of 50Hz and amplitude of 25mA. The pulse width (modulated) was linearly increased from 0 μ s to 350 μ s with an increment of 1 μ s before linearly falling from 350 μ s to 0 μ s at the same rate. Ten trials were performed for each participant. The electrodes (Physio Future International, Dimension: 5cm x 5cm) were placed on the forearm. One electrode was placed slightly higher than the medial condyle and the other over the flexor surface of the forearm. During the experiment, the volunteers were asked to rest their arms on the table, supported against gravity, without any constraints or contraptions. The MPU6050 sensor was placed on the dorsal region of the palm using a velcro band to capture the motion. The raw data from the inertial sensor was sampled at 100Hz and retrieved through the serial interface for storage and analysis.

B. Data Analysis

The raw position data from the inertial sensor was exported to Matlab(Mathworks, USA) for computational analysis. The response of the wrist flexors (angular position) along the flexion-extension axis was estimated from the accelerometer and gyroscope data using the complementary filter algorithm. The Matlab System Identification Toolbox was used to estimate the Wiener model between pulse width (an input) and angular position of the wrist flexor (output).

The proposed method cannot be experimented by combining with any kind of entity computant intelligence, fuzzy logic method and genetio. Algorithm strategie. As the novelty of the proposed work is demonstrated in the Matlab environment with the data received from the sensor placed on the voltmeter wrist flexion by modelling with the wiener based model which are the constitution of two different sensors units such as gyroscopoe and accelometer. As the data obtained with content amplitude with pulse width varing with data received from the sensor unit. As data from sensor unit is collected with the variours trails, with the considerable two volunteer and different sets, hence the discussion and data analysis is limited to the two numerical analysis.

Identification of Model

The Wiener model is illustrated as a block structure in Fig 1. The input to this model is the pulse width, and the output is the computed angular position.

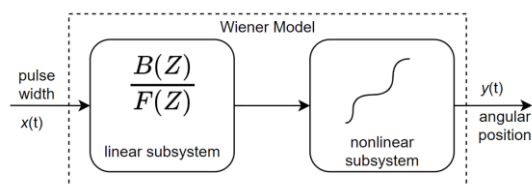


Fig 1: Structure of the Wiener model. A dynamic linear system cascaded with a static non linear system [11]

The dynamic linear subsystem in the model is described by the Equation 1, and the nonlinear subsystem is defined by Equation 2 in this work.

$$\frac{B(Z)}{F(Z)} = \frac{b_0 + b_1 z^{-1} + \dots + b_n z^{-n}}{a_0 + a_1 z^{-1} + \dots + a_n z^{-n}} \quad (1)$$

$$y_{sigmoid}(x) = \frac{a}{1 + \exp\left(-\frac{(x-x_0)}{b}\right)} \quad (2)$$

For each subject, three separate iterations of identification and validation were performed. In each iteration, the data from the ten trials were randomly split into an identification set (8) and a validation set (2). A Wiener structure with a first-order linear model cascaded with a sigmoid nonlinear subsystem was implemented to estimate the model. After the identification, the model was validated [17]. The performance of the model is indicated by the % best-fit metric, which is computed as shown in Equation 3. This process is repeated for each iteration. The estimated model with the highest % best fit was selected.

$$\%BestFit = \left(1 - \frac{|y(t) - \hat{y}(t)|}{|y(t) - \bar{y}(t)|}\right) * 100 \quad (3)$$

where $\hat{y}(t)$ is the model output, $\bar{y}(t)$ is the mean of $y(t)$ and $y(t)$ is the response.

Computation of the Angular Position Along Flexion Extension Axis

The placement of the IMU on the dorsal surface of the palm enabled the measurement of the angular position during flexion along the flexion extension axis of the wrist.

Fig 2 illustrates the implementation of the complementary filter. The complementary filter combines the high pass filtered estimation from the gyroscope and the low pass filtered estimation from accelerometers [18]. The implementation of the complementary filter to estimate the angular position is described by the Equations (4, 5, 6). The value of α is 0.95, and the value of β is 0.05, where α and β are the weights of the complementary filter.

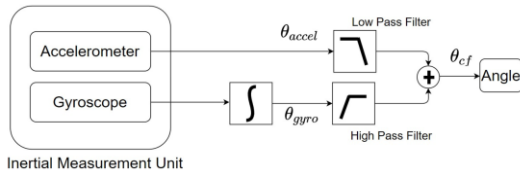


Fig 2: Complementary filter approach

In the complementary filter approach is illustrated in Fig. 2, the low pass filter allows the lower frequency signals of the accelerometer and the High pass filter will allow the higher frequency signals of the gyroscope. The sum of these two signals are fed to find the angle.

Figures and Tables should be numbered as follows

$$\theta_{cf}(t) = \alpha * \theta_{gyro}(t) + \beta * \theta_{accel}(t) \quad (4)$$

$$\theta_{accel}(t) = \arctan\left(\frac{x_g}{\sqrt{(y_g^2 + z_g^2)}}\right) \quad (5)$$

$$\theta_{gyro}(t) = g_y * \delta T + \theta_{cf}(t - 1) \quad (6)$$

C. Nonlinear PID Controller Design

PID is an effective feedback-based control method that is used to maintain the output of a system at the desired level. In this work, the PID controller is designed to regulate the pulse width of the applied electrical stimulation (with constant amplitude) to induce and maintain the desired angular position during flexion.

The nonlinear PID approach proposed in [19] has been adopted in this work. The nonlinear PID control method for the Wiener model is illustrated in Fig 3. The PID controller encounters only the linear portion of the Wiener model by compensating the nonlinear part of the Wiener model with its inverse in the feedback path. The nonlinear inverse function is also introduced before the error computation part to ensure that the output is directly compared with the inverse values. The PID controller regulates the pulse width (control signal) at its output by operating on the error signal computed as the difference between the measured and desired angular position during stimulation (calculated after applying the inverse function).

Experimental Process and Data Analysis

The PID controller for the wrist flexor model (subject-specific) was designed and simulated on Simulink. A Saturation block was introduced at the output depending on the maximum angular position measured during the previous experiment. The sample time of the controller was set to 0.02s. The PID controller was tuned to establish the controller parameters (Kp, Ki, Kd, N) to optimize for the least root mean squared error between the desired and measured angles. After the controller was tuned, real-time positional control experiments were conducted on the healthy volunteers. The controller was tested against two reference angles (a) flexion at 30° and (b) 50° for the subjects. The reference angles are considered such that it does not exceed the maximum angular displacement measured during the identification experiment. Each test was performed five times for a duration of 10s each. The performance of the controller was quantified using rise time, settling time with a tolerance of 5%, % overshoot, and the root mean square error between the desired and actual angles.

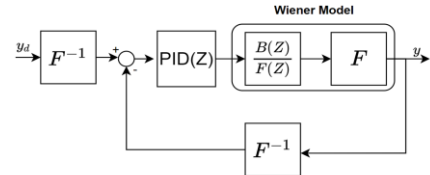


Fig 3: Nonlinear PID controller design for a wiener model. y_d is the desired setpoint, y is the measured output, F is the nonlinear function, F^{-1} is the inverse of the nonlinear function and $\frac{B(Z)}{F(Z)}$ is the linear function.

Wiener model is explained in the fig 3. It consists of a negative feedback loop, that enables a part of the y to be

feedback to maintain the stability. As mentioned, y_d is the desired setpoint, PID is nonlinear controller design for a wiener model and the measured output is y .

III. RESULTS

A. Identification of Wiener Model

Table-1 shows the characteristics of the measured angle when the pulse width modulated stimulation was applied. The characteristics in the table indicate the average maximum angular displacement response recorded for each volunteer and the average rise time of the response acquired over ten iterations.

Table-1: Table presenting the characteristics of the response obtained when pulse width modulated stimulation was applied. The values presented are the average of ten iterations. pw_{thresh} is the value of pulse width after which the the angle began to rise.

| Subjects | Characteristics of response to stimulation | | |
|-----------|--|---------------|---------------------------|
| | Flexion Angle (°) | Rise Time (s) | Pw _{thresh} (μs) |
| Subject 1 | 64.5 | 2.48 | 153 |
| Subject 2 | 60.91 | 2.14 | 164 |

The rise time of the response obtained for S1 (2.48s) was slightly quicker than or S2 (2.14s). Additionally, the table also indicates the value of pulse width (pw_{thresh}), after which the response begins to rise. For S1 this value was at 153μs, and 164 μs for S2. The angular response started to saturate after 277 μs and 271 μs for S1 and S2. A Wiener model with a first-order linear subsystem cascaded with a nonlinear sigmoid subsystem was used to identify the dynamic response.

The parameters of the identified system are described in Table-2. Table-3 summarizes the results of the model identification and validation. The final model chosen for S1 and S2 were from the models trained for iteration 1 and 3, respectively. The average best fit rate of the final model, was 79.06%, and 78.5% respectively, for S1, and S2.

Table-2: Parameters of the wiener model. The first order linear model cascaded with the sigmoidal nonlinear model. The model is described by Equations 1 & 2.

| | Linear Model | | Nonlinear Sigmoid | | |
|----|--------------|--------------------|-------------------|------|----------|
| | B(Z) | F(Z) | B(Z) | F(Z) | B(Z) |
| S1 | 1 | $1 - 0.9837z^{-1}$ | 67.32 | 1618 | $9.09e3$ |
| S2 | 1 | $1 - 0.9821z^{-1}$ | 62.3 | 1327 | $7.87e3$ |

Table 3: The average % best fit for the identified models in each validation iteration

| Accuracy (%) best fit for each validation iteration. | | | |
|--|-------------|-------------|-------------|
| | Iteration 1 | Iteration 2 | Iteration 3 |
| Model for S1 | 79.06±1.30 | 71.26±1.00 | 57.94±9.20 |
| Model for S2 | 65.88±25.90 | 74.34±9.60 | 78.50±10.60 |

Performance of Nonlinear PID Controller

Fig 4 and Table (4,5) illustrate the performance of the controller from experiments and simulations. Small overshoots and fast settling times were observed during simulations. Large overshoots were observed during the experiments, especially when the reference angle was set to 50°. For S2, it was 10.2%, and for S1, it was 7.3%. The response obtained from both subjects showed long settling times. The rise time observed during simulations was comparatively longer than during experiments. During the experiments, the least RMS error was observed for S1 (0.63°) when the reference angle was set to 30°.

| Performance of Controller for Subject 1 and 2 – Experimental | | | | | | | | |
|--|---------------|------|------------------|------|----------------|------|-------------|-------|
| | Rise Time (s) | | Settling Time(s) | | RMSE Error (°) | | % Overshoot | |
| | 30° | 50° | 30° | 50° | 30° | 50° | 30° | 50° |
| | S1 | 0.82 | 1.43 | 2.38 | 2.32 | 0.63 | 1.08 | 5.94 |
| S2 | 1.64 | 0.97 | 1.98 | 3.02 | 2.72 | 1.82 | 3.48 | 10.20 |

Table-4: The performance of the controller quantified by the average rise time and settling time, %overshoot and RMS error from experiments.

| Performance of Controller for Subject 1 and 2 – Simulation | | | | | | | | |
|--|---------------|------|---------------|------|---------------|------|---------------|------|
| | Rise Time (s) | | Rise Time (s) | | Rise Time (s) | | Rise Time (s) | |
| | 30° | 50° | 30° | 50° | 30° | 50° | 30° | 50° |
| | S1 | 1.75 | 1.50 | 1.32 | 1.29 | 0.02 | 0.14 | 1.53 |
| S2 | 1.78 | 1.51 | 1.36 | 1.30 | 0.11 | 0.18 | 1.53 | 0.50 |

Table-5: The performance of the controller quantified by the average rise time and settling time, %overshoot and RMS error from simulations.

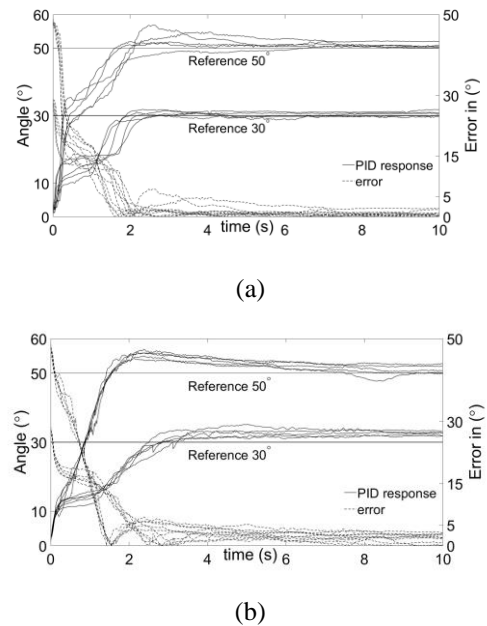


Figure 4: Simulation graph of time Vs angle for PID response and error (a) for Volunteer 1 (b) for Volunteer 2

The Analysis in regard of angel of variation among the two-difference range of angle 30° & 50° are to be illustrate along with its respective error with the response of the PID response is as shown in figure 4.

Figure illustrates the real-time nonlinear PID response (solid line) and the absolute error (dot-ted line) computed as the difference between the reference and measured angular displacement for S1(top),and S2(bottom). The controller was tested against two reference angles (30° & 50°). For both subjects, the overshoot observed while approaching 30° was less. While approaching 50° , the response was more consistent for S2 than for S1. The response while approaching 30° was more similar.

IV. DISCUSSION

The data collected for identification revealed that the measured angles appeared to have an asymmetric response during the ascending and descending phase of the pulse width modulation for the subjects. A slow rise and sharp fall characterized it. When the pulse width was varied from 0- $350\mu s$, no response was seen until a threshold value of pulse width. This threshold value was smaller for S1 ($153\mu s$) than S2 ($164\mu s$). This observation is attributed to subject-specific muscle recruitment behaviour during pulse width modulated stimulation [20]. For pulse widths greater than pw_{thresh} , the response increased with the pulse width. However, the time taken to increases was slower for S1 as compared to S2. Subsequently, as the pulse width was further increased, the response began to saturate to a steady level after a pulse width of $277\mu s$ for S1 and $271\mu s$ for S2 until the descending phase of the pulse width modulation. This trend has been previously shown in [21].

The Wiener model with the cascaded linear and nonlinear structure captured the nonlinear behavior of the wrist flexor responses. The model has a simple form and is less complex than the nonlinear models presented in [14, 20]. The average fitness of models (average of the models identified for the subjects) was 78.8%. This level of accuracy is inferior compared to the more complex nonlinear models such as the Bobet and Stein (6% error) model [12], and Hammerstein (16% error) model [22]. Simplifications introduced in the Wiener model, such as using a first-order linear model and a sigmoidal nonlinear subsystem, were carried out to simplify the controller design in the second experiment. The effects of these simplifications were evident during identification. The models were unable to capture all the dynamics accurately. Therefore, the % best fit values presented in Table 3 show significant variations across the three validation iterations. This would suggest that the predictive ability of the model was weak when tested against certain trials. Additionally, this would also indicate that the response obtained for a subject during certain trials was significantly different from the response of other trials for the same stimulation protocol.

The nonlinear PID approach adopted in this work allows for the regulation of pulse width during stimulation. The use of pulse width as the regulating variable is more favorable than

pulse amplitude with regards to the selectivity of recruitment thresholds [23]. The performance of the nonlinear PID controller in this work is encouraging. Although the controller generated a significant overshoot, the root mean squared error at steady state was small (largest RMS error was $<2.72^\circ$). This result was comparable with the controllers presented in [24, 25]. However response generated by the controller had long settling times and significant overshoot. The results obtained from simulations and experiments were different. The controller response in simulations had very little overshoot and short settling times. However, the rise time was much faster in the real-time experiments than in simulations. Errors induced due to modeling inaccuracies contribute to this observation. A more compact model that could capture all dynamics would assist in developing a better controller. However, complex models would require sophisticated control strategies as discussed in [25]. This aspect of modeling and controller design is a trade-off that needs to be investigated further.

Limitations: In this work, ten trials were carried out per subject to obtain information for modeling. Involuntary responses induced by subjects during stimulation affect the experimental data. Increasing the number of trials per subject would help analyze these effects if any. Additionally, with a rich data set, training and validation of the model can be performed more efficiently.

Directions for Future Scope: In the future enhancement of the proposed work, which provides the scope for the implementing other nonlinear model structures would possibly allow for developing more accurate models. More accurate models will assist in designing better controllers. Additionally, the nonlinear PID controller response must be optimized, in accordance with the Lyapunov function or the result with the differential equation are quite challenging to directions of fututre scope. For the intended task and needs to be designed consciously, keeping in mind response times, overshoots, disturbances and external perturbations. Moreover, in the future, experiments need to be conducted on subjects with upper limb paralysis to focus on developing practical solutions.

V. CONCLUSION

A closed-loop FES system was implemented in this work to enable angular positional control during wrist flexion by regulating the stimulation pulse width. The response of the wrist flexors to the pulse width modulated stimulation was described by a Wiener model. The model has a simple structure and comprises a first-order linear subsystem cascaded with a nonlinear sigmoid subsystem. The average fitness of the model to describe the dynamics was 78.8%. Subsequently, a nonlinear PID controller was designed based on the identified Wiener model to enable angular positional control. The angular position estimated using a complementary filter algorithm was used to provide feedback to the controller. The controller was tested in real-time against two reference angles on the healthy volunteers. Although the controller generated significant overshoot and settling times, the average RMS error at steady state was

small ($<2.72^\circ$). Reducing errors caused due to modelling and optimizing the controller will improve the performance of the presented closed-loop FES system.

Acknowledgements: The research conducted in this paper was partly supported by a BIRAC grant BT/AIR0945/PACE-19/19.

References:

- [1] Forrester, Larry W., Lewis A. Wheaton, and Andreas R. Luft. "Exercise-mediated locomotor recovery and lower-limb neuroplasticity after stroke." *Journal of Rehabilitation Research & Development* 45.2 (2008).
- [2] Peckham, P. Hunter, and Jayme S. Knutson. "Functional electrical stimulation for neuromuscular applications." *Annu. Rev. Biomed. Eng.* 7 (2005): 327-360.
- [3] Doucet, Barbara M., Amy Lam, and Lisa Griffin. "Neuromuscular electrical stimulation for skeletal muscle function." *The Yale journal of biology and medicine* 85.2 (2012): 201.
- [4] Moreno Juan C., Antonio J. Del Ama, Ana de Los Reyes-Guzmán, Angel Gil-Agudo, Ramón Ceres, and José L. Pons. "Neurobotic and hybrid management of lower limb motor disorders: a review." *Medical & biological engineering & computing* 49.10 (2011): 1119-1130.
- [5] Sheffler, Lynne R., and John Chae. "Neuromuscular electrical stimulation in neurorehabilitation." *Muscle & Nerve: Official Journal of the American Association of Electrodiagnostic Medicine* 35.5 (2007): 562-590.
- [6] Egglestone, S.R., Axelrod, L., Nind, T., Turk, R., Wilkinson, A., Burridge, J., Fitzpatrick, G., Mawson, S., Robertson, Z., Hughes, A.M. and Ng, K.H. "A design framework for a home-based stroke rehabilitation system: Identifying the key components." *2009 3rd International Conference on Pervasive Computing Technologies for Healthcare*. IEEE, 2009.
- [7] Lynch, Cheryl L., and Milos R. Popovic. "Functional electrical stimulation." *IEEE control systems magazine* 28.2 (2008): 40-50.
- [8] Schauer, Thomas. "Sensing motion and muscle activity for feedback control of functional electrical stimulation: Ten years of experience in Berlin." *Annual Reviews in Control* 44 (2017): 355-374.
- [9] Hill, Archibald Vivian. "The heat of shortening and the dynamic constants of muscle." *Proceedings of the Royal Society of London. Series B-Biological Sciences* 126.843 (1938): 136-195.
- [10] Ojanguren, Eukene Imatz. *Neuro-fuzzy Modeling of Multi-field Surface Neuroprostheses for Hand Grasping*. Springer, 2019.
- [11] Bobet, Jacques, E. Roderich Gossen, and Richard B. Stein. "A comparison of models of force production during stimulated isometric ankle dorsiflexion in humans." *IEEE transactions on neural systems and rehabilitation engineering* 13.4 (2005): 444-451.
- [12] Wilson, Emma, Emiliano Rustighi, Philip L. Newland, and Brian R. Mace. "A comparison of models of the isometric force of locust skeletal muscle in response to pulse train inputs." *Biomechanics and modeling in mechanobiology* 11.3 (2012): 519-532.
- [13] Bobet, Jacques, Richard B. Stein, and M. Namik Oguztoreli. "A linear time-varying model of force generation in skeletal muscle." *IEEE transactions on biomedical engineering* 40.10 (1993): 1000-1006.
- [14] Ding, Jun, Anthony S. Wexler, and Stuart A. Binder-Macleod. "A mathematical model that predicts the force–frequency relationship of human skeletal muscle." *Muscle & Nerve: Official Journal of the American Association of Electrodiagnostic Medicine* 26.4 (2002): 477-485.
- [15] Raghavendra, P., Viswanath Talasila, Vinay Sridhar, and Ramesh Debur. "Triggering a Functional Electrical Stimulator Based on Gesture for Stroke-Induced Movement Disorder." *Computing and Network Sustainability*. Springer, Singapore, 2017. 61-71.
- [16] Ang Wei Tech, Pradeep K. Khosla, and Cameron N. Riviere. "Kalman filtering for real-time orientation tracking of handheld microsurgical instrument." *2004 IEEE/RSJ International Conference on Intelligent Robots and Systems (IROS)(IEEE Cat. No. 04CH37566)*. Vol. 3. IEEE, 2004.
- [17] Fourati, Hassen, Nouredine Manamanni, Lissan Afilal, and Yves Handrich. "Complementary observer for body segments motion capturing by inertial and magnetic sensors." *IEEE/ASME transactions on Mechatronics* 19.1 (2012): 149-157.
- [18] Raghavendra, , Padmanabha, Madhusudhana Sachin, P. S. Srinivas, and Viswanath Talasila. "Design and development of a real-time, low-cost IMU based human motion capture system." *Computing and Network Sustainability*. Springer, Singapore, 2017. 155-165.
- [19] Erol, F. *Nonlinear PID control using Hammerstein or Wiener models*. Diss. M. Sc. Thesis. Faculty of Electrical Engineering, Eindhoven University of Technology, The Netherlands, 1999.
- [20] Ferrarin, Maurizio, Francesco Palazzo, Robert Rienen, and Jochen Quintern. "Model-based control of FES-induced single joint movements." *IEEE Transactions on Neural systems and rehabilitation engineering* 9.3 (2001): 245-257.
- [21] Kuhn, Andreas, Thierry Keller, Marc Lawrence, and Manfred Morari. "A model for transcutaneous current stimulation: simulations and experiments." *Medical & biological engineering & computing* 47.3 (2009): 279-289.
- [22] Le., Fengmin, Ivan Markovsky, Christopher T. Freeman, and Eric Rogers. "Identification of electrically stimulated muscle models of stroke

patients." *Control Engineering Practice* 18.4 (2010): 396-407.

- [23] Kesar, Trisha, Li-Wei Chou, and Stuart A. Binder-Macleod. "Effects of stimulation frequency versus pulse duration modulation on muscle fatigue." *Journal of Electromyography and Kinesiology* 18.4 (2008): 662-671
- [24] Rouhani, Hossein, Michael Same, Kei Masani, Ya Qi Li, and Milos R. Popovic. "PID controller design for FES applied to ankle muscles in neuroprosthesis for standing balance." *Frontiers in neuroscience* 11 (2017): 347.
- [25] Lynch, Cheryl L. *Closed-Loop Control of Electrically Stimulated Skeletal Muscle Contractions*. University of Toronto, 2011.

Author Contributions

S J Mahendra and Abhilash G Dutt carried out the design and development and execution of experiments. Vishwanath Talasila provided creative inputs and assisted in the writing of the manuscript. Source of Funding: The research conducted in this paper was partly supported by a BIRAC grant BT/AIR0945/PACE-19/19.

Creative Commons Attribution License 4.0 (Attribution 4.0 International, CC BY 4.0)

This article is published under the terms of the Creative Commons Attribution License 4.0

https://creativecommons.org/licenses/by/4.0/deed.en_US